Spatial Assessment of PM10 Concentrations and Population Exposure in the Emilia-Romagna Region (Italy): A Geostatistical Approach

Beatrice Manganelli[1], Rachele Vanessa Gatto[2(✉)], Simone Corrado[2], and Benedetto Manganelli[2]

[1] Department of Civil, Chemical, Environmental and Materials Engineering (DICAM), University of Bologna, Via Terracini 28, 40121 Bologna, Italy
[2] Department of Engineering (DIING), University of Basilicata, Viale Dell'Ateneo Lucano, Potenza, Italy
{rachelevanessa.gatto,simone.corrado, benedetto.manganelli}@unibas.it

Abstract. Airborne particulate matter remains one of the most critical environmental pollutants affecting urban and regional air quality, with significant implications for public health and territorial sustainability. This study investigates the spatial distribution of annual mean PM10 concentrations and associated population exposure patterns across the provinces of Parma, Reggio Emilia, Modena, and Bologna, located in a representative portion of the Emilia-Romagna region (Northern Italy), within the broader environmental context of the Po Valley, one of Europe's most critical air-pollution hotspots. The analysis is based on official monitoring data from the regional air-quality network and applies a geostatistical interpolation approach to reconstruct the spatial continuity of PM10 concentrations beyond fixed observation points. An experimental semivariogram and ordinary kriging was used to generate a continuous concentration surface at 1 km spatial resolution, together with the corresponding uncertainty map. The interpolated PM10 surface was then spatially integrated with high-resolution ISTAT population data in order to estimate the resident population exposed to different concentration classes. The findings highlight a well-defined spatial structure, with elevated PM10 concentrations in the central lowland urban system and lower levels in mountainous areas, reflecting significant variability among the main urban centers within the study area. The study highlights the relevance of geographically informed exposure assessment as a support tool for air-quality governance, spatial planning, and targeted environmental policies.

Keywords: environmental pollutants · exposure assessment · spatial planning

© The Author(s), under exclusive license to Springer Nature Switzerland AG 2027
O. Gervasi et al. (Eds.): ICCSA 2026 Workshops, LNCS 16761, pp. 526–541, 2027.
https://doi.org/10.1007/978-3-032-30527-5_34

1 Introduction

Airborne particulate matter (PM) represents one of the most critical components of air pollution and remains a major concern for both environmental monitoring and public health protection [1]. The increasing attention to PM dynamics is strongly related to the well-established link between pollutant exposure and adverse health effects, particularly respiratory and cardiovascular diseases [2]. PM is widely acknowledged as a key risk factor, especially in densely populated and highly urbanized areas.

In recent years, growing emphasis has been placed on the spatial dimension of exposure, highlighting two key implications. First, there is a need to complement traditional emission-reduction policies with place-based strategies aimed at limiting pollutant accumulation and reducing exposure in vulnerable urban contexts. Second, it becomes essential to identify the role of spatial characteristics, such as settlement morphology, industrial location patterns, and environmental assets, in influencing the distribution and concentration of PM [3].

Within this framework, green infrastructure (GI) has emerged as a relevant element in urban air-quality regulation. In addition to its ecological and climatic functions, GI contributes to pollutant mitigation through both deposition and aerodynamic processes [4]. Vegetation can enhance the capture of airborne particles due to its high surface-to-volume ratio, while deposition efficiency varies according to species-specific characteristics such as leaf morphology, size, porosity, and canopy structure. Moreover, GI can influence local airflow dynamics, thereby affecting the dispersion and redistribution of atmospheric pollutants [5].

These dynamics are particularly significant in urbanized and infrastructurally complex territories, where high population density [2], intense traffic flows, industrial activities, and land-use transformations generate persistent air-quality pressures. At the global scale, urbanization is expected to continue rapidly, with approximately 68% of the world's population projected to live in urban areas by 2050 (https://www.un.org/uk/desa/68-world-population-projected-live-urban-areas-2050-says-un). Simultaneously, the expansion of urbanized surfaces and the reduction of green spaces are exacerbating environmental stressors, including urban heat island effects and declining air quality [2].

Current international estimates indicate that a substantial share of the global urban population is exposed to air pollution levels exceeding the health-based thresholds recommended by the World Health Organization (WHO), including the annual PM10 guideline value of 15 $\mu g/m^3$ (https://www.un.org/sustainabledevelopment/blog/2016/05/).

Although particulate matter may originate from natural processes such as soil resuspension, marine aerosols, and volcanic emissions, anthropogenic sources dominate in urban and peri-urban contexts. These include vehicular traffic, industrial activities, and biomass combustion [6].

In Italy, according to the National Emissions Inventory developed by ISPRA (Italian Institute for Environmental Protection and Research) (http://www.sinanet.isprambiente.it/it/sia-ispra/serie-storiche-emissioni), the residential sector accounted for approximately 40% of primary PM10 emissions in 2011, followed by transport activities, which contributed about 24%, with more than two-thirds attributable to road traffic. Industrial

processes represented approximately 19% of emissions, while farming accounted for around 11%. Notably, nearly 90% of PM10 emissions from residential heating were associated with biomass combustion.

Within this broader context, the Po Valley in Northern Italy is recognized as one of the most critical air pollution hotspots in Europe (EEA, 2020). Its geomorphological configuration, characterized by a closed basin, limited atmospheric ventilation, and frequent stagnation episodes, favors the accumulation and persistence of particulate matter. Numerous studies have highlighted the significant implications of these conditions for public health and life expectancy [2, 5–11].

The Emilia-Romagna region, located in the central-eastern sector of the Po Basin, constitutes a particularly relevant case study within this context. The region is characterized by high population density, extensive urbanization, major industrial and logistics systems, and widespread agricultural and manufacturing activities, all of which contribute to a strong anthropogenic pressure on air quality [7].

In addition, approximately 24% of PM10 emissions in Emilia-Romagna have been attributed to road transport (ARPAE, 2022), confirming the relevance of mobility-related emissions within the regional emission structure.

For these reasons, this study focuses on the Emilia-Romagna region as representative and policy-relevant territorial context for investigating the spatial distribution of PM10 concentrations and associated population exposure patterns. In particular, the analysis addresses the regional-scale annual PM10 concentrations in relation to the settlement structure and spatial distribution of the resident population, with the aim of supporting Decision Makers with geographically informed exposure assessment[12].

The analysis focuses on the provinces of Parma, Reggio Emilia, Modena, and Bologna, which represent the central urban-industrial corridor of the Emilia plain. The year 2021 was selected because it represents the most recent year with complete validated PM10 and ISTAT population datasets available at comparable spatial resolution.

A detailed reconstruction of PM10 spatial distribution, combined with a fine-scale estimation of the exposed population and contextualized through emission-source contributions, provides a robust basis for orienting targeted mitigation policies toward areas where local air-quality improvements may generate the greatest public-health benefits. In this regard, the results show a clear concentration of pollutants within the lowland basin downstream of the Apennine system, confirming the role of geomorphological and atmospheric conditions in shaping pollutant accumulation. However, the analysis also reveals a non-linear relationship between population concentration and exposure intensity. In particular, although Bologna represents the most populated urban centre in the study area, it does not fall within the highest PM10 exposure class, unlike Modena and Reggio Emilia. This finding suggests that local exposure patterns are not determined solely by demographic concentration, but also by the interaction of settlement structure, mobility-related emissions, urban form, and territorial context. Such evidence supports the need for geographically differentiated and place-based policies aimed at improving air quality through locally adapted mitigation strategies. In this sense, Bologna constitutes a particularly relevant case, as it has recently promoted policy actions aligned with the Sustainable Development Goals and progressively integrated these objectives into its territorial governance and planning instruments.

2 Study Area, Data and Methodology

2.1 Case Study

The Po Valley is widely recognized as a major air-pollution hotspot in Europe (Fig. 1) and sustained exposure to ambient pollutants in this region has been linked to adverse public-health outcomes, including reduced life expectancy [13].

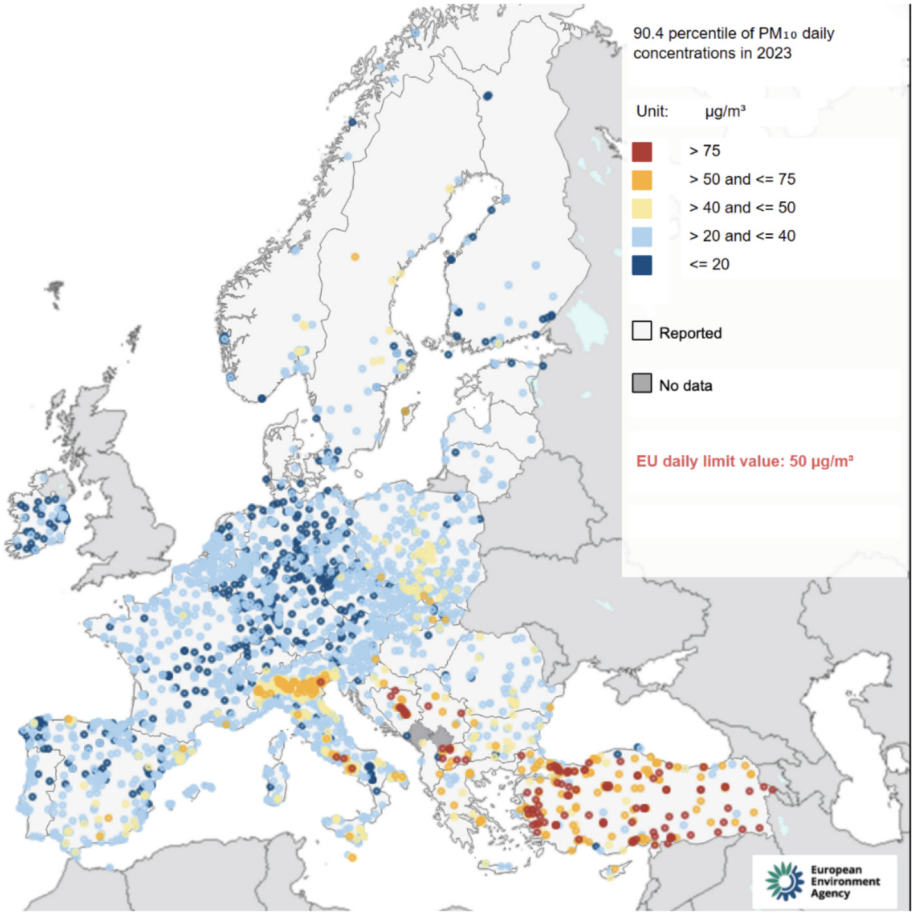

Fig. 1. The map shows the 90.4th percentile of daily PM_{10} concentrations recorded in 2023 at monitoring stations across Europe, expressed in $\mu g/m^3$. Source: European Environment Agency (EEA).

This study concentrates on the Emilia-Romagna region in Italy, which constitutes a salient case within the Po Basin, given the joint influence of relatively high population density, substantial industrial activity, pronounced urban concentration, and intensive agricultural and manufacturing production (eea.europa.eusnpambiente.it, 08/01/2026).

These pressures are further shaped by the area's geomorphological context; in particular, the enclosed basin topography and relatively weak atmospheric ventilation can facilitate pollutant build-up and prolong their residence in the local environment.

Recent monitoring data underscore both progress and ongoing issues in the region's cities concerning population exposed to PM10 (Fig. 2). PM10 annual average concentrations have generally declined or stabilized in the last 15–20 years, now usually staying below the EU annual limit of 40 $\mu g/m^3$ [10]. The 2022 annual mean PM10 was about 29–30 $\mu g/m^3$ at urban background sites in Parma and Reggio Emilia, 30–36 $\mu g/m^3$ in Modena, and around 23–27 $\mu g/m^3$ in Bologna, all within legal limits and indicative of a long-term downward trend compared to the early 2000s (when many sites averaged well above 40 $\mu g/m^3$). These improvements reflect better vehicle emissions standards, shifts from heavy fuel use, and regional policies.

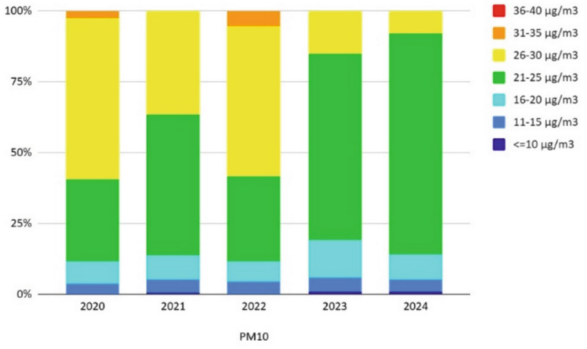

Fig. 2. Regional population exposed to annual mean concentrations of PM10. Source: ARPAE

However, daily PM10 pollution peaks continue to be problematic. Under EU standards, the 24-h average PM10 concentration should not exceed 50 $\mu g/m^3$ on more than 35 days in a year. This daily limit was frequently violated in the 2000s across the Po Valley, and while the frequency of exceedances has declined, it remains a critical issue in the cited cities. In 2022, 12 out of 43 monitoring stations in Emilia-Romagna recorded more than 35 high-PM10 days [13]. Urban centers in the central Po Valley zone saw the highest exceedances: for instance, *Modena*'s Giardini station endured 75 exceedance days (the worst in the region), *Reggio Emilia*'s Timavo station had 64**,** and *Parma*'s Montebello station 46 days beyond the 50 $\mu g/m^3$ threshold.

By contrast, in 2022, none of Bologna's PM monitoring stations surpassed the 35-day limit. Legislative standards currently lag behind health guidelines: the World Health Organization's latest recommendations (PM10 24-h guideline of 45 $\mu g/m^3$, and annual 15 $\mu g/m^3$) are far more stringent than the EU's limits (eea.europa.eu, 08/01/2026).

If these tighter limits are adopted (as proposed for 2030 in the new EU air quality directive), most Po Valley cities would be out of compliance, indicating the need for further pollution reduction acts.

To manage exceedances, regional authorities adopt short-term mitigation measures (traffic restrictions, biomass burning limits) during forecasted high-pollution episodes,

especially under the Pan-European air quality plan for the Po Basin (https://www.arpae.it/it/notizie/prosegue-lallerta-smog-in-4-province-della-regione). This includes coordinated efforts among Po Valley regions (acknowledging that "air has no boundaries" and a basin-wide approach is needed), covering sectors from transport and residential heating to agriculture (e.g. ammonia emission reductions to curb secondary PM). The regional Air Quality Plan (PAIR 2030) under development reflects these priorities, aiming to ensure sustained compliance and prepare for stricter future standards.

2.2 Data

PM10

This analysis uses an official air-quality monitoring dataset that reports PM10 levels across the Emilia-Romagna region, and it focuses on the provinces of Parma, Reggio Emilia, Modena, and Bologna (Fig. 3).

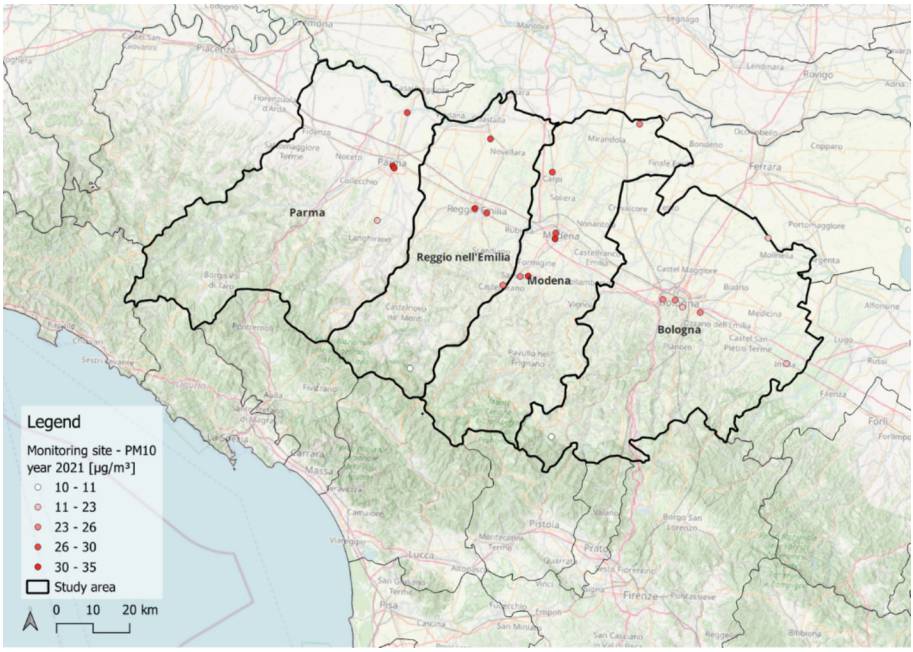

Fig. 3. Map of the study area: the provinces of Parma, Reggio Emilia, Modena and Bologna (Emilia-Romagna, Northern Italy). Black boundaries delineate the study area, while colored points represent PM_{10} monitoring stations. Symbols are classified according to annual mean PM10 concentrations recorded in 2021 ($\mu g/m^3$).

The data came from the regional air-quality monitoring network run by ARPAE (the Regional Agency for Prevention, Environment and Energy of Emilia-Romagna) and were provided in a table (Fig. 4).

The dataset is made up of on-site observations gathered from fixed monitoring stations, and the measurements are generally reliable and have been formally validated by

station_eu_code	id_regione	id_provinc	id_comune	station_co	Regione	Provincia	Comune	nome_staz	tipo_zona	tipo_stazio	TIPO	Lon	Lat	yy	n	sup50	sup45	media_yy
IT1910A	8	34	8034010	803409	Emilia-Rom	Parma	Colorno	SARAGAT	SUBURBAN	FONDO	SF	1E+07	4,5E+07	2008	277	27	34	28
IT1910A	8	34	8034010	803409	Emilia-Rom	Parma	Colorno	SARAGAT	SUBURBAN	FONDO	SF	1E+07	4,5E+07	2009	317	37	45	31
IT1910A	8	34	8034010	803409	Emilia-Rom	Parma	Colorno	SARAGAT	SUBURBAN	FONDO	SF	1E+07	4,5E+07	2010	352	28	36	27
IT1910A	8	34	8034010	803409	Emilia-Rom	Parma	Colorno	SARAGAT	SUBURBAN	FONDO	SF	1E+07	4,5E+07	2011	334	52	75	34
IT1910A	8	34	8034010	803409	Emilia-Rom	Parma	Colorno	SARAGAT	SUBURBAN	FONDO	SF	1E+07	4,5E+07	2012	338	42	63	31
IT1910A	8	34	8034010	803409	Emilia-Rom	Parma	Colorno	SARAGAT	SUBURBAN	FONDO	SF	1E+07	4,5E+07	2013	333	31	43	28
IT1910A	8	34	8034010	803409	Emilia-Rom	Parma	Colorno	SARAGAT	SUBURBAN	FONDO	SF	1E+07	4,5E+07	2014	345	29	41	27
IT1910A	8	34	8034010	803409	Emilia-Rom	Parma	Colorno	SARAGAT	SUBURBAN	FONDO	SF	1E+07	4,5E+07	2015	357	47	63	30
IT1910A	8	34	8034010	803409	Emilia-Rom	Parma	Colorno	SARAGAT	SUBURBAN	FONDO	SF	1E+07	4,5E+07	2016	355	27	30	27
IT1910A	8	34	8034010	803409	Emilia-Rom	Parma	Colorno	SARAGAT	SUBURBAN	FONDO	SF	1E+07	4,5E+07	2017	360	69	81	33
IT1910A	8	34	8034010	803409	Emilia-Rom	Parma	Colorno	SARAGAT	SUBURBAN	FONDO	SF	1E+07	4,5E+07	2018	359	24	35	28
IT1910A	8	34	8034010	803409	Emilia-Rom	Parma	Colorno	SARAGAT	SUBURBAN	FONDO	SF	1E+07	4,5E+07	2019	360	32	43	28
IT1910A	8	34	8034010	803409	Emilia-Rom	Parma	Colorno	SARAGAT	SUBURBAN	FONDO	SF	1E+07	4,5E+07	2020	360	49	54	28
IT1910A	8	34	8034010	803409	Emilia-Rom	Parma	Colorno	SARAGAT	SUBURBAN	FONDO	SF	1E+07	4,5E+07	2021	361	36	50	28
IT1910A	8	34	8034010	803409	Emilia-Rom	Parma	Colorno	SARAGAT	SUBURBAN	FONDO	SF	1E+07	4,5E+07	2022	360	33	55	30
IT1912A	8	34	8034014	803411	Emilia-Rom	Parma	Fidenza	LEOPARDI	Urbana	Fondo	UF	1E+14	4,5E+14	2008	238	21	33	28
IT1912A	8	34	8034014	803411	Emilia-Rom	Parma	Fidenza	LEOPARDI	Urbana	Fondo	UF	1E+14	4,5E+14	2009	318	38	45	29
IT1912A	8	34	8034014	803411	Emilia-Rom	Parma	Fidenza	LEOPARDI	Urbana	Fondo	UF	1E+14	4,5E+14	2010	339	34	43	26
IT1911A	8	34	8034018	803410	Emilia-Rom	Parma	Langhiranc	BADIA	RURALE	FONDO	RF	1E+07	446575	2009	266	5	7	19
IT1911A	8	34	8034018	803410	Emilia-Rom	Parma	Langhiranc	BADIA	RURALE	FONDO	RF	1E+07	446575	2010	346	14	23	20
IT1911A	8	34	8034018	803410	Emilia-Rom	Parma	Langhiranc	BADIA	RURALE	FONDO	RF	1E+07	446575	2011	359	16	23	22
IT1911A	8	34	8034018	803410	Emilia-Rom	Parma	Langhiranc	BADIA	RURALE	FONDO	RF	1E+07	446575	2012	360	11	13	21
IT1911A	8	34	8034018	803410	Emilia-Rom	Parma	Langhiranc	BADIA	RURALE	FONDO	RF	1E+07	446575	2013	348	5	6	17
IT1911A	8	34	8034018	803410	Emilia-Rom	Parma	Langhiranc	BADIA	RURALE	FONDO	RF	1E+07	446575	2014	329	5	8	16
IT1911A	8	34	8034018	803410	Emilia-Rom	Parma	Langhiranc	BADIA	RURALE	FONDO	RF	1E+07	446575	2015	354	6	10	21
IT1911A	8	34	8034018	803410	Emilia-Rom	Parma	Langhiranc	BADIA	RURALE	FONDO	RF	1E+07	446575	2016	356	8	14	20
IT1911A	8	34	8034018	803410	Emilia-Rom	Parma	Langhiranc	BADIA	RURALE	FONDO	RF	1E+07	446575	2017	361	29	37	25

Fig. 4. The main characteristics of the PM10 monitoring stations included in the analysis.

the institution. PM10 levels are given in $\mu g\ m^{-3}$, in line with the units used in European air-quality regulations.

Population

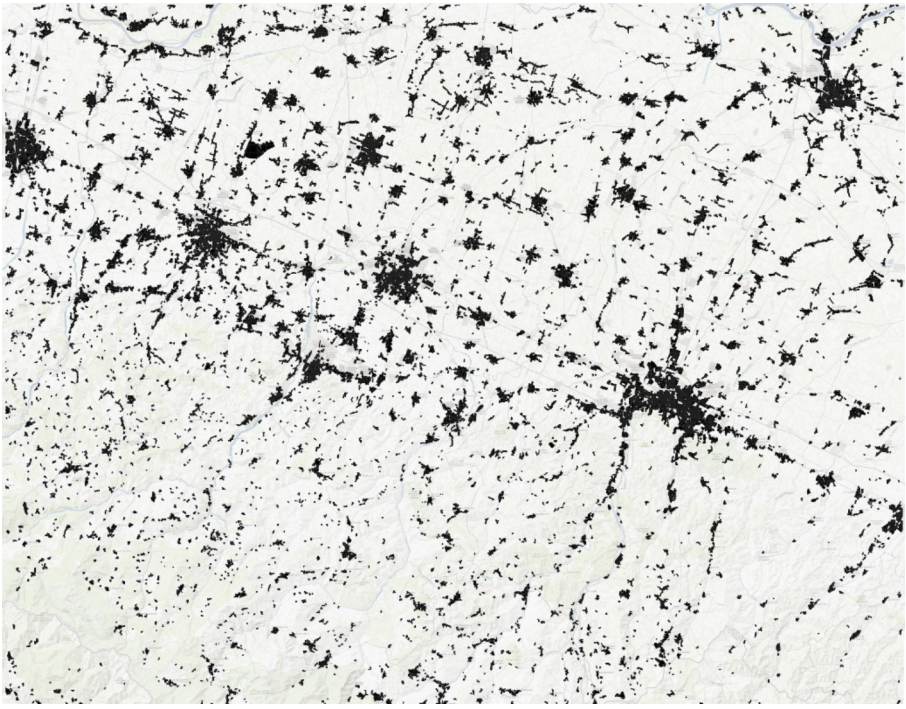

Fig. 5. Spatial Population data from ISTAT.

Population data of 2021 were obtained from the ISTAT Population and Housing Census database (Fig. 5). At the sub-municipal scale, this provides a highly detailed spatial representation of the resident population and enables the dissemination of statistical indicators at finest territorial scales.

2.3 Methodology

Traditional air quality monitoring networks provide accurate measurements at fixed locations but are inherently limited in their ability to resolve spatial continuity or to characterize pollutant levels in areas lacking direct observations. To overcome these limitations, data-driven methods have been widely adopted to reconstruct and analyze the spatial distribution of PM10 concentrations.

The interpolation was implemented using SGeMS (Stanford Geostatistical Modeling Software) [14]**.** Monitoring station data were imported as a point dataset, and a regular grid covering the study area was generated to support spatial estimation.

Ordinary kriging was selected due to the absence of a known global mean and the assumption of second-order stationarity. The final kriging outputs consist of continuous PM10 concentration surfaces and associated estimation variance maps, enabling the identification of pollution gradients and uncertainty patterns.

Once the map of the annual mean PM10 distribution for 2021 had been generated at a spatial resolution of 1km × 1km, it was spatially intersected with ISTAT population data referring to residential settlement clusters. To facilitate the interpretation of exposure patterns, the annual mean PM10 concentration map was reclassified into four concentration classes (<15 $\mu g/m^3$, 15–20 $\mu g/m^3$**,** 20–25 $\mu g/m^3$, and 25–30 $\mu g/m^3$). These classes were then used to estimate the exposure in terms of resident population related to different levels of air pollution exposure. This procedure is based on the association of PM10 concentration values with the spatial distribution of resident population across the study area.

3 Results

3.1 Spatial Structure of PM10 Concentrations

The experimental semivariogram computed from the 22 monitoring stations in the study area reveals a clear spatial dependence of annual PM10 concentrations across the whole territorial system. As expected in a lowland basin such as the Po Valley, nearby stations tend to show similar concentration values, while differences progressively increase with distance.

Directional semivariograms calculated along the four principal orientations (0°, 45°, 90°, and 135°) exhibit some variability in both shape and range (Fig. 6). In particular, a slightly more structured behaviour can be observed along the East–West direction, suggesting a potential directional influence on spatial continuity. However, these differences are not sufficiently consistent to support a robust anisotropic model. The directional curves appear irregular and affected by noise, likely due to the limited number of station pairs available in each direction and the uneven spatial distribution of the monitoring network, which is denser in urban areas and sparser in peripheral zones.

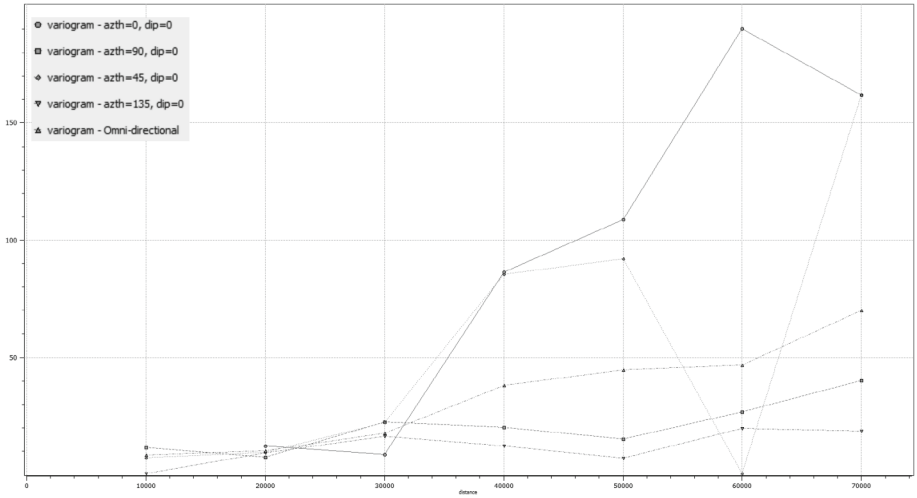

Fig. 6. The experimental variograms of 2021 PM10 concentrations computed for four principal directions (azimuths 0°, 45°, 90°, and 135°).

Given these limitations, the omnidirectional experimental variogram was considered more reliable, as it incorporates all available point pairs and provides a statistically more stable representation of spatial dependence. The omnidirectional variogram shows a rapid increase at short distances, followed by a gradual transition towards a plateau, indicating the presence of spatial correlation over several tens of kilometres.

Among the tested theoretical models (exponential, spherical, and Gaussian), the Gaussian model provided the best overall fit, effectively capturing both the smooth increase at short lag distances and the transition towards the sill. The fitted model is characterised by a nugget effect of approximately 8 ($\mu g/m^3$)2, corresponding to local residual differences of about 2.8 $\mu g/m^3$, indicating limited but non-negligible small-scale variability and/or measurement uncertainty. The sill is approximately 36 ($\mu g/m^3$)2, representing the structured component of spatial variance. This implies that PM10 concentrations may differ by approximately 6 $\mu g/m^3$ between distant locations beyond the spatial correlation range. The estimated range is about 55 km, suggesting that PM10 concentrations remain spatially correlated over relatively large distances. This result is consistent with the atmospheric behaviour of the Po Valley, were limited ventilation and basin morphology favour pollutant persistence and regional coherence.

3.2 Interpolated PM10 Surface and Uncertainty

Based on the fitted Gaussian variogram model, ordinary kriging was applied to generate a continuous surface of annual PM10 concentrations at a spatial resolution of 1 km × 1 km. This resolution allows the reconstruction of spatial gradients at the sub-provincial scale while maintaining consistency with the available monitoring data.

The interpolated PM10 map (Fig. 7) reveals a spatial pattern consistent with both the distribution of monitoring stations and known emission hotspots.

Higher concentration values, generally exceeding 25 $\mu g/m^3$, are observed in correspondence with the main urban and industrial areas, where traffic density and anthropogenic activities are more intense. These high-value clusters are primarily located along the central lowland belt of the region.

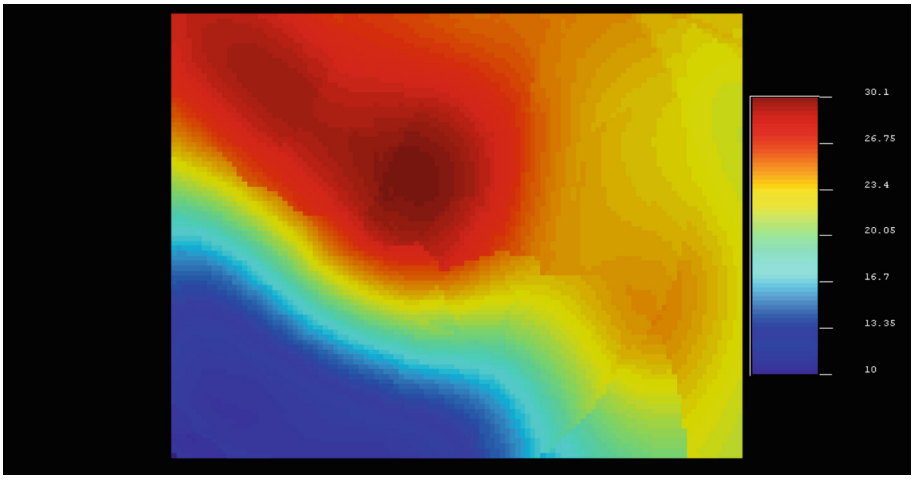

Fig. 7. Ordinary kriging interpolation of 2021 PM_{10} concentrations.

In areas characterised by a higher density of monitoring stations, the interpolated surface displays more pronounced local variability, closely reflecting observed measurements. Conversely, in peripheral and mountainous areas, where monitoring stations are sparse, the kriging surface appears smoother. This is a typical outcome of geostatistical interpolation under limited data conditions, where estimates tend to be more influenced by the overall spatial structure rather than local observations.

The kriging variance map (Fig. 8) provides a spatially explicit representation of estimation uncertainty. Lower variance values are observed in areas with a dense monitoring network, indicating higher confidence in the interpolated estimates. In contrast, variance increases significantly in areas located far from monitoring stations. This spatial pattern reflects both the geometry of the monitoring network and the estimated variogram range. Peripheral areas, particularly in the southern mountainous sectors and in the north-eastern part of the study area, show the highest uncertainty, highlighting the limitations of the current monitoring configuration and the need for caution when interpreting interpolated values in these zones.

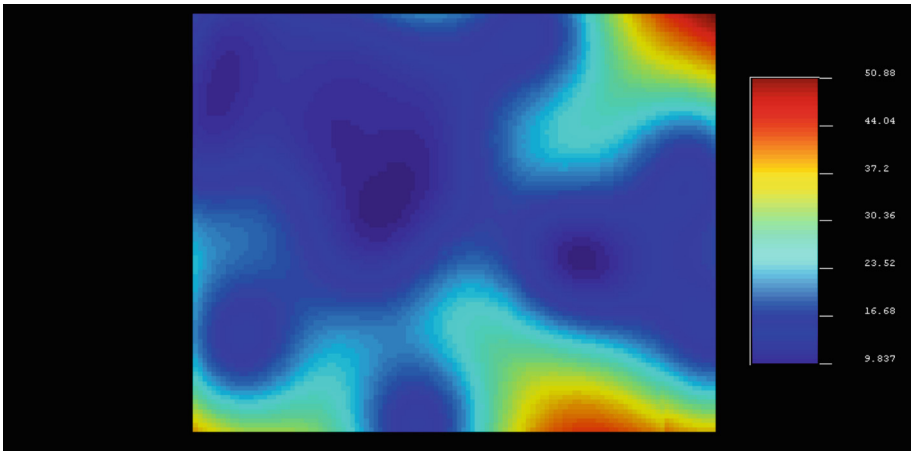

Fig. 8. Spatial distribution of kriging variance for annual PM_{10} concentrations

3.3 Spatial Distribution of Population Exposure

The integration of the interpolated PM10 surface with ISTAT population data enables the assessment of population exposure across different concentration classes. The results highlight a strong territorial polarization, with the majority of the resident population concentrated within the 20–25 $\mu g/m^3$ and 25–30 $\mu g/m^3$ classes (Fig. 9).

	<15	15 > x > 20	20>x>25	25>30	tot
Bologna	0	0	382.935,94	0	382.935,94
Modena	0	0	0	173.324,97	173.324,97
Reggio nell'Emilia	0	0	0	158.323,19	158.323,19
Parma	0	0	2.851,99	140.332,5	143.184,49
Ferrara	0	0	114.944,18	0	114.944,18
Carpi	0	0	0	66.410,19	66.410,19
Sassuolo	0	0	69	40.148,23	40.217,23
Casalecchio di Reno	0	0	37.267,1	0	37.267,1
Formigine	0	0	0	33.333,75	33.333,75
Cento	0	0	30.862,39	240,33	31.102,72
San Lazzaro di Savena	0	0	30.413	0	30.413
Imola	0	0	29.034,64	0	29.034,64
Castelfranco Emilia	0	0	0	28.708,47	28.708,47
Valsamoggia	0	440,21	9.202,56	16.688,94	26.331,71
Scandiano	0	0	362,61	23.352,06	23.714,67
San Giovanni in Persiceto	0	0	68,04	23.188,08	23.256,12
Vignola	0	0	0	22.985,39	22.985,39
Mirandola	0	0	0	22.222,71	22.222,71
Correggio	0	0	0	21.950,52	21.950,52
Zola Predosa	0	0	18.369,11	83,76	18.452,87
Casalgrande	0	0	0	17.626,79	17.626,79
Fiorano Modenese	0	0	0	17.230,56	17.230,56
Castel Maggiore	0	0	17.011,03	0	17.011,03
Castel San Pietro Terme	0	0	16.795,63	0	16.795,63
Viadana	0	0	0	16.198,05	16.198,05
Maranello	0	0	0	15.856,6	15.856,6
Finale Emilia	0	0	11.262,95	4.396,16	15.659,11
Pianoro	0	0	15.005,25	0	15.005,25
Nonantola	0	0	0	14.777,93	14.777,93
Budrio	0	0	14.457,39	0	14.457,39
Castelnuovo Rangone	0	0	0	14.379,24	14.379,24
Castellarano	0	0	4.948,34	9.281,93	14.230,27
Molinella	0	0	14.120,43	0	14.120,43

Fig. 9. Population exposure across different concentration classes annual PM_{10} concentrations.

The main urban centres of the region are almost entirely associated with medium-to-high PM10 levels (Fig. 10). Bologna, the most populated municipality, falls entirely within the 20–25 $\mu g/m^3$ class, with approximately 382,936 inhabitants exposed within this range. Similarly, Ferrara, Casalecchio di Reno, San Lazzaro di Savena, and Imola are predominantly included in the same class, indicating a widespread exposure to intermediate concentration levels across the metropolitan and peri-urban system.

A more critical situation emerges in the 25–30 $\mu g/m^3$ class, which includes several major urban and productive centres of the Emilia plain. Modena, Reggio nell'Emilia, and Parma show a large share of their population within this range, together with numerous medium-sized municipalities such as Carpi, Formigine, Castelfranco Emilia, Mirandola, Correggio, and Vignola. This confirms that the highest PM10 levels are not limited to isolated hotspots but characterize a broad and densely populated territorial system. In contrast, the lowest exposure classes (<15 $\mu g/m^3$ and 15–20 $\mu g/m^3$) are mainly associated with mountain and foothill municipalities along the Apennine belt. In these areas, lower settlement density and more favourable dispersion conditions result in significantly reduced PM10 concentrations. Municipalities such as Alto Reno Terme, Castelnovo ne' Monti, Fanano, Ventasso, and Frassinoro show a substantial proportion of their population within these lower concentration ranges.

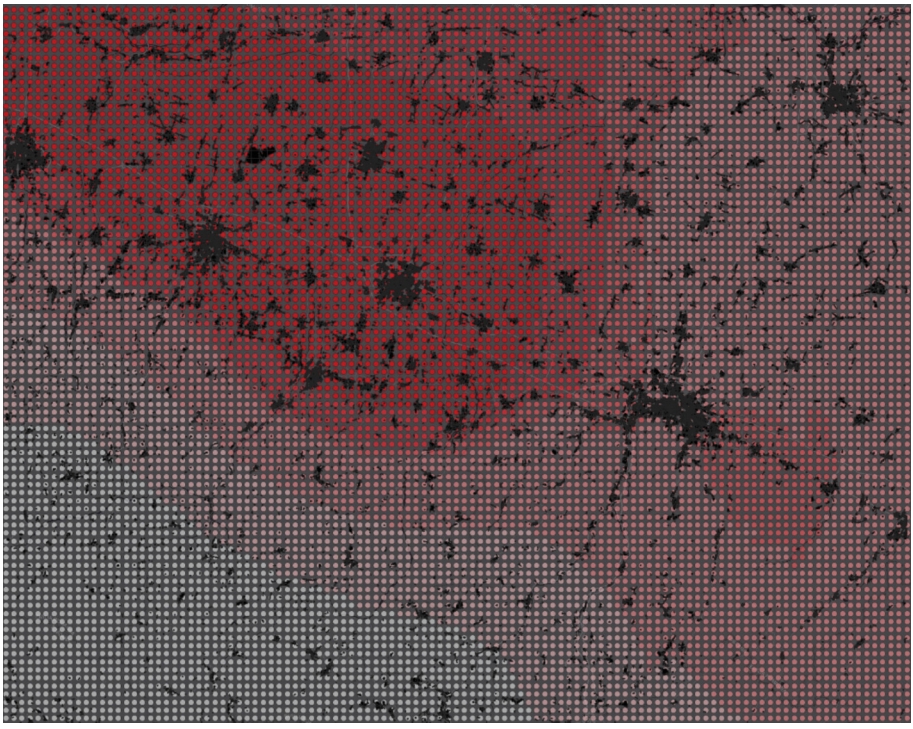

Fig. 10. Spatial distribution of kriging variance for annual PM_{10} concentrations and urban residential distributions.

3.4 Synthesis of Spatial Patterns

Overall, the results demonstrate that PM10 concentrations in the study area exhibit a well-defined spatial structure at the regional scale. The use of an omnidirectional Gaussian variogram model proved to be a robust and physically consistent choice, given the limited and uneven distribution of monitoring stations. The kriging-based maps successfully capture both the spatial distribution of concentrations and the associated uncertainty, providing a coherent framework for interpreting PM10 dynamics. When combined with population data, these results highlight spatial relations between air pollution levels, settlement patterns, and territorial structure.

In particular, the analysis shows that population exposure is strongly concentrated in the central lowland urban system, where both pollutant levels and demographic density are highest (i.e. Parma, Modena, Sassuolo, Reggio Emilia), while lower exposure levels are mainly confined to mountainous south-west municipalities (Fig. 11).

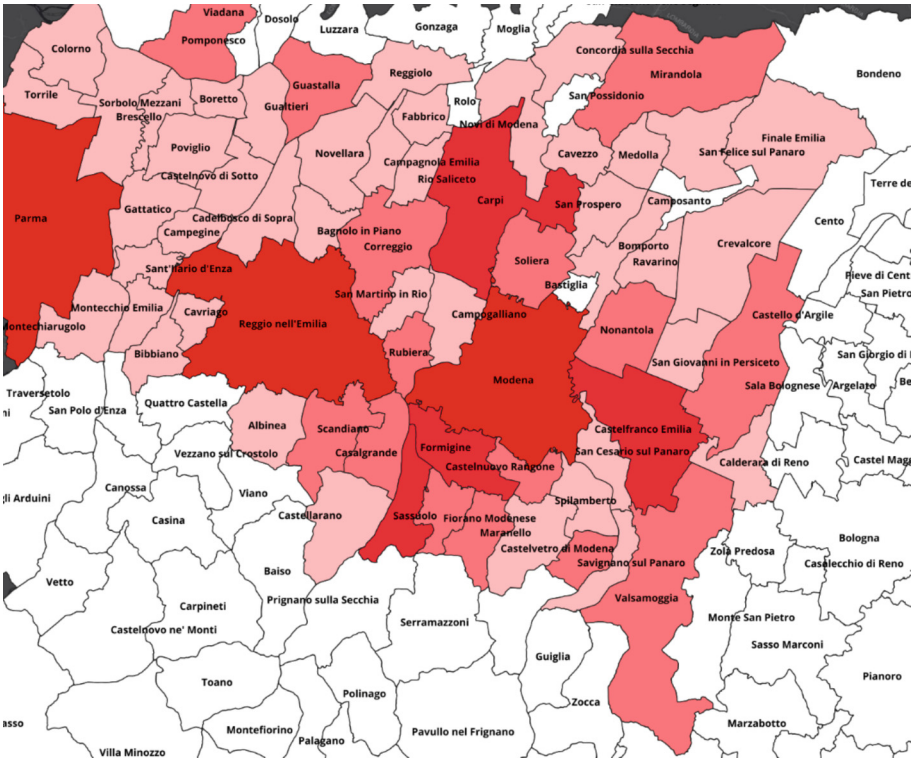

Fig. 11. Municipalities entirely included in the 25–30 $\mu g/m^3$ PM10 concentration class are highlighted in red, whereas municipalities with the largest exposed population are represented in dark red.

This confirms that PM10 exposure in the region is not randomly distributed, but structurally embedded within the geography of urbanization in the region.

4 Discussion

The results provide a spatially explicit interpretation of annual PM10 concentrations and population exposure across the study area, highlighting a clear territorial organization of air-pollution patterns within the Emilia-Romagna sector of the Po Valley. Overall, the analysis confirms the presence of a marked concentration of pollutants within the lowland basin, where geomorphological conditions, atmospheric stability, and the structure of urbanized and productive systems contribute to the persistence of PM10 accumulation.

At the same time, the findings suggest that the relationship between pollutant concentration and exposed population is not merely linear, nor can it be explained exclusively by the demographic size of urban centres. In this regard, the case of Bologna is particularly significant. Although Bologna represents the most populated urban nucleus within the study area, it does not fall within the highest PM10 concentration class identified in the analysis. However, a very large share of its resident population remains exposed to intermediate concentration levels, particularly within the 20–25 $\mu g/m^3$ range. This result is highly relevant from a public-health and planning perspective, as it shows that even concentration levels below the highest observed class may still involve a very large number of exposed inhabitants when they affect major metropolitan systems.

5 Conclusions

This study explored the spatial distribution of annual PM10 concentrations and associated population exposure patterns within a representative portion of the Emilia-Romagna region, using a geostatistical interpolation framework integrated with high-resolution population data. The results show that PM10 concentrations exhibit a well-defined spatial structure, with higher values concentrated in the central lowland urban system and lower levels in mountainous and peripheral areas.

The integration of concentration map with population data makes it possible to move beyond a purely descriptive reading of pollution patterns and to identify those territorial contexts where air-quality conditions may generate the greatest exposure burden for residents. In this sense, the analysis demonstrates that the most densely populated urban centres are not necessarily those falling within the highest PM10 concentration class. Bologna represents the clearest example of this pattern: despite not belonging to the most critical concentration class, it concentrates a very high number of exposed inhabitants due to its demographic weight and urban structure.

This finding is particularly relevant for environmental governance, as it underlines the importance of considering both pollutant intensity and exposed population in the design of local mitigation strategies.

A detailed reconstruction of PM10 spatial distribution, combined with a fine-scale estimation of the resident population exposed and interpreted in light of emission-source contributions, can provide a robust basis for orienting targeted environmental policies toward the areas where mitigation actions may produce the greatest collective benefit. In this perspective, the results support the relevance of place-based and geographically differentiated interventions, capable of addressing local pollution dynamics more effectively [4].

Consequently, the findings emphasize the importance of targeted policy actions, such as the expansion of urban green spaces, the adoption of cleaner technologies, and the strengthening of public transportation system[4]. Integrating tree-planting strategies with sustainable urban planning initiatives may contribute to reducing pollutant levels while also improving accessibility to green areas. To maximize effectiveness, afforestation efforts should prioritize high-efficiency PM-absorbing tree species, particularly in high-traffic and environmentally critical urban sectors [6].

Moreover, considering that a substantial share of PM10 emissions is likely associated with the civil sector, especially residential heating, mitigation strategies [15] should also address the improvement of heating systems and the progressive transition toward more efficient and less emissive energy solutions, including district heating where applicable [16]. In this sense, integrated environmental and urban policies may represent a key lever for improving local air quality and reducing population exposure in the most sensitive urban contexts [17].

Declaration of Generative AI and AI-Assisted Technologies in the Writing Process. During the preparation of this work the authors used ChatGPT 3.5 in order to improve the readability of parts of the text. After using this tool/service, the authors reviewed and edited the content as needed and take full responsibility for the content of the publication.

Data Availability. Data will be made available on request.

References

1. Slini, T., Kaprara, A., Karatzas, K., Moussiopoulos, N.: PM10 forecasting for Thessaloniki. Greece. Environ. Modell. Softw. **21**, 559–565 (2006). https://doi.org/10.1016/j.envsoft.2004.06.011
2. Cocchi, D., Greco, F., Trivisano, C.: Hierarchical space-time modelling of PM10 pollution. Atmos. Environ. **41**, 532–542 (2007). https://doi.org/10.1016/j.atmosenv.2006.08.032
3. Sloss, L.L., Smith, I.M.: PM10 and PM2.5: an international perspective. Fuel Process. Technol. **65–66**, 127–141 (2000). https://doi.org/10.1016/S0378-3820(99)00081-8
4. Islam, A., Pattnaik, N., Moula, Md.M., Rötzer, T., Pauleit, S., Rahman, M.A.: Impact of urban green spaces on air quality: a study of PM10 reduction across diverse climates. Sci. Total Environ. **955**, 176770 (2024). https://doi.org/10.1016/j.scitotenv.2024.176770
5. Baek, S., Kim, J., Kang, J.: Impact of green infrastructure on PM10 in port-adjacent residential complexes: a finite volume method-based computational fluid dynamics study. Sustain. Cities Soc. **115** (2024). https://doi.org/10.1016/j.scs.2024.105815
6. Queiroz Diniz Oliveira, M.C., Maura de Miranda, R., de Fátima Andrade, M., Kumar, P.: Impact of urban green areas on air quality: an integrated analysis in the metropolitan area of São Paulo. Environ. Pollut. **372** (2025). https://doi.org/10.1016/j.envpol.2025.126082
7. Ragosta, M., D'emilio, M., Casaletto, L., Telesca, V.: A statistical procedure for analyzing the behavior of air pollutants during temperature extreme events: the case study of Emilia-Romagna region (northern Italy). Appl. Sci. (Switz.) **11** (2021). https://doi.org/10.3390/app11178266
8. Shtein, A., et al.: Estimating daily PM2.5 and PM10 over Italy using an ensemble model. Environ. Sci. Technol. **54**, 120–128 (2020). https://doi.org/10.1021/acs.est.9b04279

9. Bonaventura, L., Castruccio, S., Crippa, P., Lonati, G.: Geostatistical estimate of PM10 concentrations in Northern Italy: validation of kriging reconstructions with classical and flexible variogram models (2008)
10. Bartzis, J.G., Kalimeri, K.K., Sakellaris, I.A.: Environmental data treatment to support exposure studies: the statistical behavior for NO2, O3, PM10 and PM2.5 air concentrations in Europe. Environ. Res. **181** (2020). https://doi.org/10.1016/j.envres.2019.108864
11. Beloconi, A., Chrysoulakis, N., Lyapustin, A., Utzinger, J., Vounatsou, P.: Bayesian geostatistical modelling of PM10 and PM2.5 surface level concentrations in Europe using high-resolution satellite-derived products. Environ. Int. **121**, 57–70 (2018). https://doi.org/10.1016/j.envint.2018.08.041
12. Perez, P., Reyes, J.: An integrated neural network model for PM10 forecasting. Atmos. Environ. **40**, 2845–2851 (2006). https://doi.org/10.1016/j.atmosenv.2006.01.010
13. Fabbi, S., Veratti, G., Bigi, A., Ghermandi, G.: Air quality (PM 10) scenarios resulting from the expansion of hydrogen fuel cell electric vehicle in Emilia-Romagna (Northern Italy). In: 21st International Conference on Harmonisation within Atmospheric Dispersion Modelling for Regulatory Purposes (2022)
14. Remy, N.: S-GeMS: the stanford geostatistical modeling software: a tool for new algorithms development. In: Leuangthong, O., Deutsch, C.V (eds.) Geostatistics Banff 2004, pp. 865–871. Springer, Dordrecht (2005). https://doi.org/10.1007/978-1-4020-3610-1_89
15. Murgante, B., Borruso, G., Balletto, G., Castiglia, P., Dettori, M.: Why Italy first? Health, geographical and planning aspects of the COVID-19 outbreak. Sustain. (Switz.). **12** (2020). https://doi.org/10.3390/su12125064
16. Stadlober, E., Hörmann, S., Pfeiler, B.: Quality and performance of a PM10 daily forecasting model. Atmos. Environ. **42**, 1098–1109 (2008). https://doi.org/10.1016/j.atmosenv.2007.10.073
17. Zhu, L., Huang, X., Shi, H., Cai, X., Song, Y.: Transport pathways and potential sources of PM10 in Beijing. Atmos. Environ. **45**, 594–604 (2011). https://doi.org/10.1016/j.atmosenv.2010.10.040